18

Optimum Design of Balanced Surface Acoustic Wave Filters using Evolutionary Computation

Kiyoharu Tagawa
School of Science and Engineering, Kinki University
Japan

1. Introduction

Surface Acoustic Wave (SAW) filters are small, rugged and cost-competitive mechanical band-pass filters with amazing frequency response characteristics. Therefore, SAW filters have played an important role as a key device in various mobile and wireless communication systems such as personal digital assistants (PDAs) and cellular phones (Campbell, 1998). Recently, the balanced SAW filter becomes widely used in the modern Radio Frequency (RF) circuits of cellular phones. That is because the balanced SAW filter can provide not only the band-pass filtering function but also some external functions, namely, the unbalance-balance signal conversion, the impedance conversion and so on. In other words, if we use balanced SAW filters in a modern RF circuit, we can reduce the number of the components of the modern RF circuit, as well as their mounted area (Meier et al., 2001). As a result, we can miniaturize the modern RF circuit of a cellular phone.

The frequency response characteristics of SAW filters including balanced one are governed primarily by their geometrical structures, namely, the configurations of Inter-Digital Transducers (IDTs) and Shorted Metal Strip Arrays (SMSAs) reflectors fabricated on piezoelectric substrates (Hashimoto, 2000). Therefore, in order to realize desirable frequency response characteristics of SAW filters, we have to decide strictly their geometrical structures, which are specified by using many design parameters such as the numbers of the fingers of respective IDTs, the length of the electrodes, and so on.

Several optimum design methods which combine the optimization algorithm with the computer simulation have been reported to decide suitable structures of SAW filters (Franz et al., 1997; Tagawa et al., 2002; Goto & Kawakatsu, 2004; Tagawa et al., 2007). In these optimum design methods of SAW filters, Evolutionary Algorithms (EAs) such as Genetic Algorithm (GA) have been also used as the optimization algorithm (Prabhu et al., 2002; Meltaus et al., 2004; Tagawa et al., 2003). However, conventional optimum design methods of SAW filters have been contrived for the unbalanced SAW filter. Therefore, conventional optimum design methods can't be applied directly to the balanced SAW filter.

The primary purpose of this chapter is to demonstrate the usage of the latest Evolutionary Computation (EC) technique in a real-world application, namely, the optimum design of balanced SAW filters. In the proposed optimum design method of balanced SAW filters, Differential Evolution (DE) is employed as the optimization algorithm. DE is one of the most

Source: Evolutionary Computation, Book edited by: Wellington Pinheiro dos Santos,
ISBN 978-953-307-008-7, pp. 572, October 2009, I-Tech, Vienna, Austria

recent EAs for solving real-parameter optimization problems (Storn & Price, 1997). DE exhibits an overall excellent performance for a wide range of benchmark problems. Furthermore, because of its simple but powerful searching capability, DE has got numerous real-world applications (Price et al., 2005). Actually, in our prior study about the optimum design of a balanced SAW filter, it has been shown that DE is superior to a real-coded GA in both the quality of the final solution and the computational time (Tagawa, 2008).

The computer simulation technique is very important in the optimum design method of balanced SAW filters as well as the optimization algorithm. In order to evaluate the performance of the balanced SAW filter based on the computer simulation, we have to employ a reliable model. Therefore, we explain the network model of the balanced SAW filter in detail (Tagawa, 2007). First of all, we show the equivalent circuit model of the balanced SAW filter. Then we transform the equivalent circuit model into the network model according to the balanced network theory (Bockelman & Eisenstadt, 1995).

The rest of this chapter is organized as follows. In the section 2, the basic structure and the principle of the balanced SAW filter are described briefly. The modeling and the simulation methodologies of the balanced SAW filter are also explained. In the section 3, the structural design of balanced SAW filters is formulated as an optimization problem. In the section 4, the decision variables of the optimization problem, which correspond to the various design parameters of balanced SAW filters, are embedded in the regularized continuous search space of DE. Then the procedure of a classic DE known as "DE/rand/1/bin" is described in detail. In the section 5, the structural design of a practical balanced SAW filter is formulated into two types of optimum design problems. Then the classic DE is applied to the respective optimum design problems. Furthermore, the results of computational experiments are shown and discussed. Finally, some conclusions are offered in the section 6.

2. Balanced surface acoustic wave filter

2.1 Basic structure and principle

A balanced SAW filter consists of several components, namely, Inter-Digital Transducers (IDTs) and Shorted Metal Strip Array (SMSA) reflectors fabricated on a piezoelectric substrate. Figure 1 illustrates a typical structure of the balanced SAW filter that consists of five components: one transmitter IDT (IDT-T), two receiver IDTs (IDT-R) and two SMSAs. Furthermore, port-1 is an input-port, while port-2 and port-3 are output-ports.

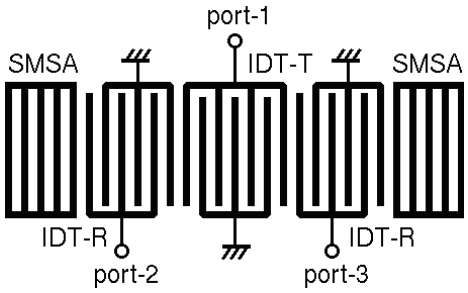

Fig. 1. Typical structure of the balanced SAW filter

Each of IDTs is composed of some pairs of electrodes called fingers and used for Surface Acoustic Wave (SAW) excitation and detection. The balanced SAW filter is a kind of the

resonator-type SAW filter that has a symmetrical structure centering IDT-T. The input electric signals of port-1 are converted to acoustic signals in IDT-T. Then the acoustic signals are resonated between two SMSAs. Furthermore, the acoustic signals are reconverted to electric signals in IDT-Rs. Even though the balanced SAW filter had a symmetrical structure, the polarities of two IDT-Rs' electrodes are designed to be opposite. Therefore, a pair of port-2 and port-3 connected to respective IDT-Rs provides a balanced output-port.

2.2 Modeling and simulation

For analyzing the frequency response characteristics of SAW filters based on the computer simulation, we have to utilize their reliable models. Therefore, in order to evaluate the performance of the balanced SAW filter, we present the network model (Tagawa, 2007). The network model of the balanced SAW filter is derived from the conventional equivalent circuit model according to the balanced network theory (Bockelman & Eisenstadt, 1995).

The equivalent circuit model of a balanced SAW filter is made up from the equivalent circuit models of its components, namely, IDTs and SMSAs. First of all, Fig. 2 shows examples of the structures of IDTs with N-pair of fingers. The behavior of each IDT in Fig. 2 can be analyzed by using a three-port circuit model illustrated in Fig. 3 (Kojima & Suzuki, 1992). In the circuit model in Fig. 3, port-A and port-B are acoustic-signal ports, while port-C is an electric-signal port. Circuit elements appeared in Fig. 3, namely, transconductances A_{10} and A_{20}, impedances Z_1 and Z_2, admittance Y_m, and capacitance C_T are given as follows.

$$\begin{cases} A_{10} &= \tanh\left(\dfrac{\gamma_s}{2}\right)\tanh\left(N\gamma_s\right) \\ A_{20} &= \mp A_{10} \\ Z_1 &= \dfrac{1}{R_0 F_s}\tanh\left(N\gamma_s\right) \\ Z_2 &= \dfrac{1}{R_0 F_s}\left(\dfrac{1}{\sinh\left(2N\gamma_s\right)}\right) \\ Y_m &= \dfrac{2F_s}{R_0}\tanh\left(\dfrac{\gamma_s}{2}\right)\left[2N-\tanh\left(\dfrac{\gamma_s}{2}\right)\tanh\left(N\gamma_s\right)\right] \\ C_T &= NC_{so}\dfrac{K\left(\sin\left(\eta\dfrac{\pi}{2}\right)\right)}{K\left(\cos\left(\eta\dfrac{\pi}{2}\right)\right)} \end{cases} \tag{1}$$

where, the dual sign (±) means that the minus (-) is for $2N$ being an even number as shown in Fig. 2 (a), while the plus (+) is for $2N$ being an odd number as shown in Fig. 2 (b). Furthermore, R_0 denotes the characteristic impedance. F_s is the image admittance, and γ_s is the image transfer constant. $K(z)$ is the complete elliptic integral of a real number $z \in R$.

If the electric port (port-C) is shorted in Fig. 3, the equivalent circuit model of IDT becomes the equivalent circuit model of SMSA reflector (Kojima & Suzuki, 1992). Now, because all of the components of a balanced SAW filter are connected acoustically in cascade on a piezoelectric substrate, the entire equivalent circuit model of the balanced SAW filter can be composed by linking together the acoustic-ports of their equivalent circuit models.

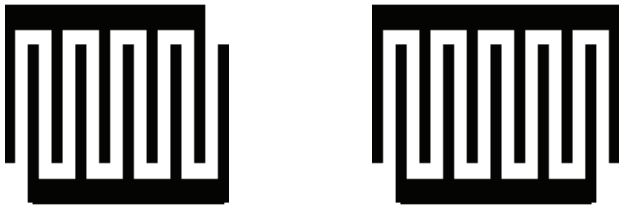

(a) *N=5* (integer) (b) *N=5.5* (half-integer)

Fig. 2. Structure of Inter-Digital Transducer (IDT) with *N*-pair of fingers

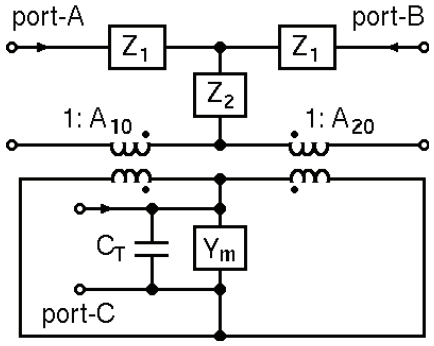

Fig. 3. Equivalent circuit model of IDT

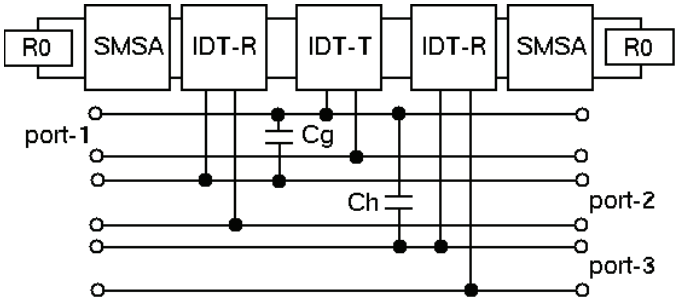

Fig. 4. Equivalent circuit model of the balanced SAW filter shown in Fig. 1

For example, the equivalent circuit model of the balanced SAW filter in Fig. 1 is given by a six-port circuit in Fig. 4, where a pair of port-2 and port-3 corresponds to the balanced output-port, while port-1 is the unbalanced input-port. Incidentally, C_h and C_g denote coupling capacitances between one IDT-T and two IDT-Rs. A serious difference between C_h and C_g causes the deterioration of the balance characteristics of the balanced SAW filter.
Terminating the three extra ports of the six-port equivalent circuit model in Fig. 4, the balanced SAW filter shown in Fig. 1 can be represented by an admittance matrix $\boldsymbol{Y}$ in (2).

$$Y = \begin{bmatrix} y_{11} & y_{12} & y_{13} \\ y_{21} & y_{22} & y_{23} \\ y_{31} & y_{32} & y_{33} \end{bmatrix} \tag{2}$$

Furthermore, considering the impedances of the input-port Z_{in} and the output-port Z_{out}, the admittance matrix $\boldsymbol{Y}$ in (2) is transformed into a scattering matrix $\boldsymbol{S}$ as shown in (3).

$$S = BA^{-1} = \begin{bmatrix} s_{11} & s_{12} & s_{13} \\ s_{21} & s_{22} & s_{23} \\ s_{31} & s_{32} & s_{33} \end{bmatrix} \tag{3}$$

where, matrixes A and B are given by using the elements of Y as follows.

$$A = \begin{bmatrix} 1+Z_{in}y_{11} & Z_{in}y_{12} & Z_{in}y_{13} \\ -Z_{out}y_{21} & 1+Z_{out}y_{22} & -Z_{out}y_{23} \\ -Z_{out}y_{31} & -Z_{out}y_{32} & 1+Z_{out}y_{33} \end{bmatrix}$$

$$B = \begin{bmatrix} 1-Z_{in}y_{11} & -Z_{in}y_{12} & -Z_{in}y_{13} \\ Z_{out}y_{21} & 1+Z_{out}y_{22} & Z_{out}y_{23} \\ Z_{out}y_{31} & Z_{out}y_{32} & 1+Z_{out}y_{33} \end{bmatrix}$$

From the scattering matrix $\boldsymbol{S}$ in (3), a three-port network model of the balanced SAW filter can be represented graphically as shown in Fig. 5 (Tagawa, 2007). In the network model in Fig. 5, nodes a_q (q=*1, 2, 3*) denote the input signals of the balanced SAW filter, while nodes b_p (*p=1, 2, 3)* denote the output signals. Scattering parameters s_{pq} on edges provide the transition characteristics from input signals a_q to output signals b_p. Furthermore, a pair of port-2 and port-3 of the network model in Fig. 5 corresponds to the balanced output-port of the balanced SAW filter in Fig. 1, while port-1 corresponds to the unbalanced input-port.

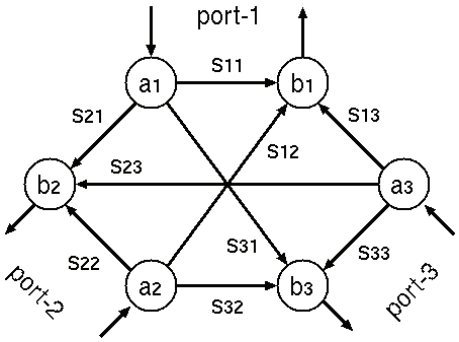

Fig. 5. Network model of the balanced SAW filter shown in Fig. 1

2.3 Balance characteristics

In the balanced SAW filter, it is desirable that the output signals b_2 and b_3 from the balanced output-port, namely, a pair of port-2 and port-3 of the three-port network model in Fig.5, have the same amplitude and 180 degrees phase difference through the pass-band. Therefore, in order to evaluate the balance characteristics of the balanced SAW filter, two

criteria are usually used (Koshino et al., 2002). The amplitude balance of the balanced SAW filter is evaluated by criterion E_1 in (4). On the other hand, the phase balance of the balanced SAW filter is evaluated by criterion E_2 in (5). In an ideal condition of the balanced SAW filter, the values of both the criteria E_1 and E_2 should become zero through the pass-band.

$$E_1 = 20\log_{10}\left(\left|s_{21}\right|\right) - 20\log_{10}\left(\left|s_{31}\right|\right) \tag{4}$$

$$E_2 = \varphi\left(s_{21}\right) - \varphi\left(s_{31}\right) + 180 \tag{5}$$

where, $\varphi(s_{pq})$ denotes the phase angle of the scattering parameter s_{pq}.

2.4 Filter characteristics

The balanced SAW filter is used as a band-pass filter. In order to evaluate the band-pass filter characteristics of the balanced SAW filter strictly, we have to segregate the differential mode signal from the common mode signal in the three-port network model in Fig. 5. Therefore, according to the theory of the balanced network (Bockelman & Eisenstadt, 1995), we reorganize the entering signals a_q (q=2, 3) and the leaving signals b_p (p=2, 3) of the balanced port, or the pair of port-2 and port-3, respectively as shown in (6) and (7). Consequently, signals a_d and b_d defined in (6) correspond to differential mode signals of the balanced SAW filter, while signals a_c and b_c defined in (7) correspond to common mode signals.

$$\begin{cases} a_d &= \dfrac{1}{\sqrt{2}}\left(a_2 - a_3\right) \\ b_d &= \dfrac{1}{\sqrt{2}}\left(b_2 - b_3\right) \end{cases} \tag{6}$$

$$\begin{cases} a_c &= \dfrac{1}{\sqrt{2}}\left(a_2 + a_3\right) \\ b_c &= \dfrac{1}{\sqrt{2}}\left(b_2 + b_3\right) \end{cases} \tag{7}$$

From the definition shown in (6) and (7), the matrix $\boldsymbol{S}$ of conventional scattering parameters in (3) can be converted into the matrix $\boldsymbol{S}_{mix}$ of mix-mode scattering parameters as follows.

$$S_{mix} = T\,S\,T^{-1} = \begin{bmatrix} s_{11} & s_{1d} & s_{1c} \\ s_{d1} & s_{dd} & s_{dc} \\ s_{c1} & s_{cd} & s_{cc} \end{bmatrix} \tag{8}$$

where, matrix $\boldsymbol{T}$ is given as follows.

$$T = \frac{1}{\sqrt{2}}\begin{bmatrix} \sqrt{2} & 0 & 0 \\ 0 & 1 & -1 \\ 0 & 1 & 1 \end{bmatrix}$$

In order to evaluate the band-pass filter characteristics of the balanced SAW filter as well as the unbalanced one (Tagawa et al., 2003), we use the above mix-mode scattering parameters instead of conventional scattering parameters. Therefore, the standing wave ratios of the input-port E_3 and the output-port E_4 can be defined respectively in (9) and (10). Also, the attenuation E_5 between the input-port and the output-port is defined as shown in (11).

$$E_3 = \frac{1+|s_{11}|}{1-|s_{11}|} \tag{9}$$

$$E_4 = \frac{1+|s_{dd}|}{1-|s_{dd}|} \tag{10}$$

$$E_5 = 20\log_{10}(|s_{d1}|) \tag{11}$$

3. Problem formulation

3.1 Design parameters

The frequency response characteristics of balanced SAW filters depend on their geometrical structures, or the configurations of their components fabricated on piezoelectric substrates. For example, in order to decide the structure of the balanced SAW filter in Fig. 1, we have to adjust nine design parameters (N_T, N_R, N_S, l_p, W, ξ, ξ_m, ρ_m, H) illustrated in Fig. 6. The design parameters N_T and N_R represent the numbers of the fingers of IDT-T and IDT-R respectively. Similarly, N_S is the number of the strips of SMSA. The design parameter l_p denotes the finger pitch of IDT. W denotes the overlap between facing electrodes. The metallization ratio of IDT ξ is defined as $\xi=l_m/l_p$ with the finger pitch l_p and the metal width of the finger l_m ($l_m<l_p$). The metallization ratio of SMSA ξ_m is also defined as $\xi_m=r_m/r_p$ with the strip pitch r_p and the metal width of the strip r_m ($r_m<r_p$). The pitch ratio of SMSA is defined as $\rho_m=r_p/l_p$ based on the finger pitch of IDT l_p. Besides, H denotes the metal thickness of electrode.

A set of design parameters describing the structure of a balanced SAW filter is represented by a vector of decision variables: $\boldsymbol{x}=(x_1, \ldots, x_D)$. Each decision variable $x_j \in \boldsymbol{x}$ ($j=1, \ldots, D$) is either a continuous value or a discrete value as shown in Fig. 6. Furthermore, the values of decision variables $x_j \in \boldsymbol{x}$ are bounded by their parametric limitations as follows.

$$x_j^L \le x_j \le x_j^U, \quad j = 1, \cdots, D \tag{12}$$

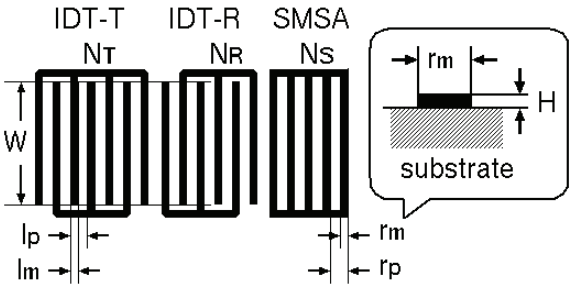

Fig. 6. Design parameters of the balanced SAW filter shown in Fig. 1

3.2 Objective function

By using the criteria E_r (r=1, …, 5) for the balanced SAW filter described in the previous section, we define the objective function to be minimized. The values of criteria E_r=$E_r(\omega, \boldsymbol{x})$ depend on both the frequency ω and the decision variable $\boldsymbol{x}$. Therefore, let Ω_p be a set of frequency points sampled from the pass-band of the balanced SAW filter. Similarly, let Ω_s be a set of frequency points sampled from the stop-band. Then we specify the desirable band-pass filter characteristics of the balanced SAW filter $E_r(\omega, \boldsymbol{x})$ (r=3, 4, 5) by their upper $U_r(\omega)$ and lower $L_r(\omega)$ bounds at $\omega \in \Omega_p$ or $\omega \in \Omega_s$. Consequently, considering the criteria of the balance characteristics $E_r(\omega, \boldsymbol{x})$ (r=1, 2) and those of filter characteristics $E_r(\omega, \boldsymbol{x})$ (r=3, 4, 5) for the balanced SAW filter, we define the objective function $f(\boldsymbol{x})$ as follows.

$$f(x) = \sum_{r=1}^{5} \frac{\alpha_r}{|\Omega_p|} f_r(x) + \frac{\alpha_6}{|\Omega_s|} f_6(x) \tag{13}$$

where, $|\Omega_p|$ and $|\Omega_s|$ denote the number of elements included in Ω_p and Ω_s respectively. Also α_r>0 (r=1, …, 6) are weighting coefficients. Functions $f_r(\boldsymbol{x})$ are given as follows.

$$\begin{cases} f_1(x) &= \sum_{\omega \in \Omega_p} E_1(\omega, x)^2 \\ f_2(x) &= \sum_{\omega \in \Omega_p} E_2(\omega, x)^2 \\ f_3(x) &= \sum_{\omega \in \Omega_p} \max\{E_3(\omega, x) - U_3(\omega), 0\} \\ f_4(x) &= \sum_{\omega \in \Omega_p} \max\{E_4(\omega, x) - U_4(\omega), 0\} \\ f_5(x) &= \sum_{\omega \in \Omega_p} \max\{L_5(\omega) - E_5(\omega, x), 0\} \\ f_6(x) &= \sum_{\omega \in \Omega_s} \max\{E_5(\omega, x) - U_5(\omega), 0\} \end{cases}$$

3.3 Optimum design problem

From the boundary constraints in (12) and the objective function in (13), the structural design of the balanced SAW filter is formulated into an optimization problem as follows.

$$\min_{x \in X} \quad f(x) \tag{14}$$

where, $\boldsymbol{X}$ denotes a set of feasible solutions that satisfy the boundary conditions in (12).

4. Differential evolution

Differential Evolution (DE) (Storn & Price, 1997) is one of the most recent EAs for solving real-parameters optimization problems. DE exhibits an overall excellent performance for a wide range of benchmark problems. Furthermore, because of its simple but powerful searching capability, DE has got numerous real-world applications (Price et al., 2005).

4.1 Representation

DE is usually used to solve the optimization problem in which the objective function to be minimized is defined on D ($D \geqq 1$) real-parameters. DE holds N_P individuals, or the candidate solutions of the optimization problem, in the population. As well as conventional real-coded GAs (Eshelman & Schaffer, 1993), every individual of DE is coded as a D-dimensional real-parameter vector. Furthermore, the i-th individual $\boldsymbol{x}_{i,g}$ ($i=1, \ldots, N_P$) included in the population of the generation g ($g \geqq 0$) is represented as follows.

$$x_{i,g} = \left(x_{1,i,g}, \cdots, x_{j,i,g}, \cdots, x_{D,i,g}\right) \tag{15}$$

As shown in the previous section 3, each decision variable $x_j \in \boldsymbol{x}$ of the optimization problem in (14) corresponds to a design parameter of the balanced SAW filter and takes either a continuous value or a discrete value. However, in order to apply DE to the optimization problem in (14), or the optimum design problem of balanced SAW filters, each of the decision variables $x_j \in \boldsymbol{x}$ ($j=1, \ldots, D$) has to be represented by a real-parameter. Therefore, we propose a new technique that converts an individual $\boldsymbol{x}_{i,g}$ into a corresponding solution $\boldsymbol{x}$.
First of all, we define the regularized continuous search space of DE as shown in (16). Each element of the individual $x_{j,i,g} \in \boldsymbol{x}_{i,g}$ is restricted within the range between 0 and 1.

$$0 \leq x_{j,i,g} \leq 1, \quad j = 1, \cdots, D \tag{16}$$

Then every decision variable of the optimization problem is embedded in the regularized continuous search space of DE defined in (16). Exactly speaking, each element $x_{j,i,g} \in \boldsymbol{x}_{i,g}$ in (16) is converted into the corresponding decision variable $x_j \in \boldsymbol{x}$ when the objective function value $f(\boldsymbol{x})$ is evaluated. If a decision variable $x_j \in \boldsymbol{x}$ takes a continuous value originally, the corresponding $x_{j,i,g} \in \boldsymbol{x}_{i,g}$ is converted into the decision variable $x_j \in \boldsymbol{x}$ as shown in (17). On the other hand, if a decision variable $x_j \in \boldsymbol{x}$ takes a discrete value with an interval e_j, the corresponding $x_{j,i,g} \in \boldsymbol{x}_{i,g}$ is converted into the decision variable $x_j \in \boldsymbol{x}$ as shown in (18).

$$x_j = \left(x_j^U - x_j^L\right) x_{j,i,g} + x_j^L \tag{17}$$

$$x_j = round\left(\frac{\left(x_j^U - x_j^L\right) x_{j,i,g}}{e_j}\right) e_j + x_j^L \tag{18}$$

where, the operator $round(z)$ rounds a real number $z \in \boldsymbol{R}$ to the nearest integer.

4.2 Procedure of differential evolution

Even though various revised DEs have been proposed (Chakraborty, 2008), we employ the classic DE named ''DE/rand/1/bin" (Storn & Price, 1997). That is because the classic DE is commonly used and powerful enough for solving real-world applications (Price et al., 2005). The procedure of the classic DE is described as follows. The genetic operators used in the classic DE, namely, the generation of an initial population in Step 1, the differential mutation in Step 4 and the binomial crossover in Step 5, will be explained later. For convenience, we represent the aforementioned conversion from an individual $\boldsymbol{x}_{i,g}$ to the corresponding solution $\boldsymbol{x}$ defined in (17) and (18) by a unified operator $\boldsymbol{x}=h(\boldsymbol{x}_{i,g})$ in Step 6. Furthermore, the stopping criterion in Step 2 is usually specified by the maximum generation.

< Classic DE >

Step 1. Randomly generate N_P individuals as an initial population. Set the generation $g=0$.

Step 2. If the stopping criterion is satisfied, output the best individual and terminate.

Step 3. For each individual $\boldsymbol{x}_{i,g}$ ($i=1, \ldots, N_P$) of the population, which is called the target vector, randomly select mutually different three individuals, $\boldsymbol{x}_{r1,g}$, $\boldsymbol{x}_{r2,g}$ and $\boldsymbol{x}_{r3,g}$.

Step 4. Generate the mutated vector $\boldsymbol{v}_{i,g}$ from the above three individuals, $\boldsymbol{x}_{r1,g}$, $\boldsymbol{x}_{r2,g}$ and $\boldsymbol{x}_{r3,g}$ ($i \neq r1 \neq r2 \neq r3$) by using the differential mutation.

Step 5. Generate the trial vector $\boldsymbol{u}_{i,g}$ ($i=1, \ldots, N_P$) by using the binomial crossover between the mutated vector $\boldsymbol{v}_{i,g}$ and the target vector $\boldsymbol{x}_{i,g}$.

Step 6. If $f(h(\boldsymbol{u}_{i,g})) \leq f(h(\boldsymbol{x}_{i,g}))$ then set $\boldsymbol{x}_{i,g+1}=\boldsymbol{u}_{i,g}$, otherwise set $\boldsymbol{x}_{i,g+1}=\boldsymbol{x}_{i,g}$.

Step 7. Set $g=g+1$ and return to Step 2.

4.3 Initialization

In Step 1 of the procedure of the classic DE, individuals $\boldsymbol{x}_{i,0}$ ($i=1, \ldots, N_P$) are generated randomly as an initial population within the search space of DE defined in (16). Therefore, each element $x_{j,i,0} \in \boldsymbol{x}_{i,0}$ ($j=1, \ldots, D$) of an individual $\boldsymbol{x}_{i,0}$ can be generated as follows.

$$x_{j,i,0} = rand_j[0,1], \quad j = 1, \cdots, D; \quad i = 1, \cdots, N_P \tag{19}$$

where, $rand_j[0, 1]$ is the random number generator that returns a uniformly distributed random number from within the range between 0 and 1. The subscript $j \in [1, D]$ indicates that a new random value is generated for each of the elements $x_{j,i,0} \in \boldsymbol{x}_{i,0}$.

4.4 Differential mutation

Differential mutation is a unique genetic operator to DE. In order to generate the mutated vector $\boldsymbol{v}_{i,g}$ in Step 4 of the procedure the classic DE, the differential mutation amplifies difference vector between $\boldsymbol{x}_{r2,g}$ and $\boldsymbol{x}_{r3,g}$, and adds the result to $\boldsymbol{x}_{r1,g}$ as shown in (20).

$$v_{i,g} = x_{r1,g} + S_F \left(x_{r2,g} - x_{r3,g} \right) \tag{20}$$

where, the scale factor $S_F \in (0, 1+]$ is a user-defined control parameter.

Applying the above differential mutation, some elements of the mutated vector $v_{j,i,g} \in \boldsymbol{v}_{i,g}$ may go out of the search space of DE defined in (16). In such a case, these illegal elements $v_{j,i,g} \in \boldsymbol{v}_{i,g}$ are remade again within the search space of DE as shown in (21).

$$v_{j,i,g} = \begin{cases} rand_j[0,1] x_{j,r1,g}, & if\left(v_{j,i,g} < 0\right) \\ 1 + rand_j[0,1]\left(x_{j,r1,g} - 1\right), & if\left(v_{j,i,g} > 1\right) \end{cases} \tag{21}$$

4.5 Binomial crossover

In order to generate the trial vector $\boldsymbol{u}_{i,g}$ in Step 5 of the procedure of the classic DE, binomial crossover, which is similar to the uniform crossover of GA, is employed. The binomial crossover between the mutated vector $\boldsymbol{v}_{i,g}$ and the target vector $\boldsymbol{x}_{i,g}$ is described as follows.

$$u_{j,i,g} = \begin{cases} v_{j,i,g}, & if\left(rand_j[0,1] \le C_R \vee j = j_r\right) \\ x_{j,i,g}, & otherwise \end{cases} \tag{22}$$

In the above binomial crossover in (22), the crossover rate $C_R \in [0, 1]$ is also a user-defined control parameter that controls the fraction of decision variables copied from the mutated vector. Furthermore, $j_r \in [1, D]$ is a randomly selected subscript of the element of the mutated vector $v_{j,i,g} \in \boldsymbol{v}_{i,g}$ and it ensures that the trial vector $\boldsymbol{u}_{i,g}$ inherits at least one element from the mutated vector $\boldsymbol{v}_{i,g}$. As a result, we can expect that the trial vector $\boldsymbol{u}_{i,g}$ is different from the target vector $\boldsymbol{x}_{i,g}$, even if we choose the crossover rate as $C_R=0$.

5. Computational experiments

5.1 Problem instance

As an instance of the optimum design problem, a suitable structure of a practical balanced SAW filter illustrated in Fig. 7 is considered. In order to restrain the reflection of acoustic wave signals between IDT-T and IDT-R, the balanced SAW filter in Fig. 7 has pitch-modulated IDTs between IDT-T and IDT-R (Kawachi, 2004). Therefore, the balanced SAW filter consists of nine components, namely, seven IDTs and two SMSAs.

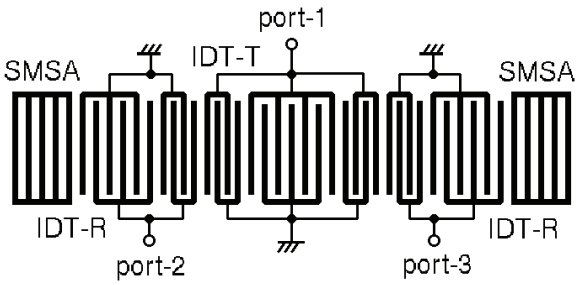

Fig. 7. Balanced SAW filter with pitch-modulated IDTs

x_j	x_j^L	x_j^U	e_j	design parameter
x_1	200	400	−	overlap between facing electrodes
x_2	10.0	20.0	0.5	number of the fingers of IDT-R
x_3	15.5	25.5	1.0	ditto of IDT-T
x_4	1.0	3.0	1.0	ditto of pitch-modulated IDT
x_5	50	150	10	number of the strips of SMSA
x_6	0.4	0.6	−	metallization ratio of IDT
x_7	0.4	0.6	−	ditto of SMSA
x_8	0.91	0.92	−	pitch ratio of pitch-modulated IDT
x_9	1.00	1.05	−	ditto of SMSA
x_{10}	1.95	2.05	−	finger pitch of IDT
x_{11}	3900	4000	−	thickness of electrode

Table 1. Design parameters of the balanced SAW filter shown in Fig. 7

In order to describe the structure of the balanced SAW filter shown in Fig. 7, eleven design parameters are chosen carefully. Table 1 shows the eleven design parameters, or the decision variables $x_j \in \boldsymbol{x}$ ($j=1, \ldots, D; D=11$) of the optimum design problem, and their upper x_j^U and lower x_j^L bounds. Furthermore, intervals e_j of design parameters x_j are also described in Table 1 if corresponding design parameters x_j have to take discrete values.
The objective function $f(\boldsymbol{x})$ in (13) is evaluated at *401* frequency points within the range between *850*[MHz] and *1080*[MHz]. The pass-band is also given by the range between *950*[MHz] and *980*[MHz]. Besides, all weighted coefficients are set as $\alpha_r=1$ $(r=1, \ldots, 6)$.

5.2 Experimental results

The program of the classic DE is realized by using MATLAB®. For evaluating the objective function values in the procedure of the classic DE, the simulator for the balanced SAW filter shown in Fig. 7 is also coded by MATLAB®. Then the classic DE is applied to the optimum design problem of the balanced SAW filter in Fig. 7. As the stopping criterion in Step 2 of the procedure of the classic DE, the maximum generation is limited to $g_{max}=100$. Also the control parameters of the classic DE are given as follows: the population size $N_P=50$, the scale factor $S_F=0.85$ and the crossover rate $C_R=0.9$. These values of the control parameters were decided through exploratory experiments in advance. Incidentally, the program of the classic DE spends about *16* minutes for one run on a personal computer.
In order to evaluate the effectiveness of the classic DE, the best solution in the final population is compared with the best solution in the initial population in Table 2. Table 2 shows the best objective function values f_{ave} averaged over *20* runs and their standard deviation σ_f. The partial function values $f_r(\boldsymbol{x}^*)$ $(r=1, \ldots, 6)$ of the objective function value $f(\boldsymbol{x}^*)$, which are related to respective criteria E_r $(r=1, \ldots, 5)$ of the balanced SAW filter, are also declared in Table 2. We can hereby confirm that the performance of the balanced SAW filter has been improved by the classic DE not only about the objective function $f(\boldsymbol{x}^*)$ but also about all the criteria E_r.

$D=11$	$g=0$		$g=g_{max}$	
	f_{ave}	σ_f	f_{ave}	σ_f
$f(\boldsymbol{x}^*)$	3.357	0.381	2.075	0.002
$f_1(\boldsymbol{x}^*)$	177.612	45.794	72.771	1.019
$f_2(\boldsymbol{x}^*)$	940.120	103.687	634.409	3.954
$f_3(\boldsymbol{x}^*)$	38.749	11.512	26.074	1.4793
$f_4(\boldsymbol{x}^*)$	39.061	12.229	27.018	1.4815
$f_5(\boldsymbol{x}^*)$	9.147	4.030	5.902	0.530
$f_6(\boldsymbol{x}^*)$	38.002	14.197	21.591	1.375

Table 2. Objective function values of the initial and the final best solutions $\boldsymbol{x}^*$ ($D=11$)

Figure 8 plots a representative example of the trajectory of the best objective function values achieved in the respective generations of the classic DE. From the results in Fig. 8, we can see that the classic DE has found the final best solution early in the searching procedure.

5.3 Extended optimum design problem

In order to utilize further the power of DE, we try to increase the degree of the design freedom in the above optimum design problem of the balanced SAW filter in Fig. 7.

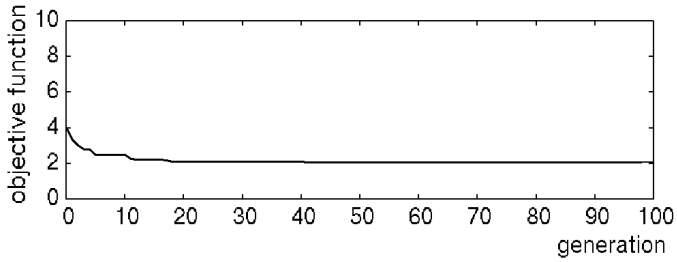

Fig. 8. Trajectory of the best objective function values (*D=11*)

The balanced SAW filter usually takes a symmetrical structure. Therefore, in the selection of the design parameters listed in Table 1, we have supposed that the balanced SAW filter in Fig. 7 takes a symmetrical structure. In other words, in the design of the balanced SAW filter, the right-side IDT-R and the left-side IDT-R have the same number of fingers. Similarly, the right-side SMSA and the left-side SMSA have the same number of stripes.

Now, in order to improve the performance of the balanced SAW filter much more, we extend the formulation of the optimum design problem. We suppose that the balanced SAW filter can take not only a symmetrical structure but also an unsymmetrical one. Then we increase the number of the design parameters $x_j \in \boldsymbol{x}$ ($j=1, \ldots, D$), which are used to describe the structure of the balanced SAW filter in Fig. 7, from *D=11* to *D=15*.

D=15	$g=0$		$g=g_{max}$	
	f_{ave}	σ_f	f_{ave}	σ_f
$f(\boldsymbol{x}^*)$	9.151	7.281	0.713	0.016
$f_1(\boldsymbol{x}^*)$	263.687	323.901	55.721	4.962
$f_2(\boldsymbol{x}^*)$	2787.312	3114.794	150.003	8.113
$f_3(\boldsymbol{x}^*)$	204.174	253.710	20.120	3.817
$f_4(\boldsymbol{x}^*)$	209.172	259.212	20.273	3.845
$f_5(\boldsymbol{x}^*)$	51.108	54.495	2.831	1.145
$f_6(\boldsymbol{x}^*)$	153.565	85.198	37.010	6.951

Table 3. Objective function values of the initial and the final best solutions $\boldsymbol{x}^*$ (*D=15*)

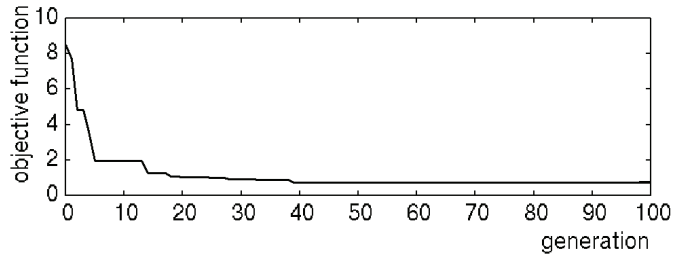

Fig. 9. Trajectory of the best objective function values (*D=15*)

By using the same values for the control parameters, the classic DE is applied to the extended optimum design problem of the balanced SAW filter. Table 3 compares the final best solution with the initial best solution in the same way with Table 2. Furthermore, Fig. 9 plots a representative example of the trajectory of the best objective function values in the

same way with Fig. 8. Comparing the results in Table 2 and Table 3, in the initial generation ($g=0$), the best solution obtained for the extended optimum design problem ($D=15$) is inferior to the best solution obtained for the original optimum design problem ($D=11$) in every function value. However, in the final generation ($g=g_{max}$), the former best solution is superior to the latter best solution. We can also confirm the above-mentioned phenomenon from the comparison of the two trajectories shown in Fig. 8 and Fig. 9 respectively.

In order to verify the results in Table 2 and Table 3, we compare the final best solution of the extended optimum design problem ($D=15$) with the final best solution of the original optimum design problem ($D=11$) in the frequency response characteristics of the balanced SAW filter. Figure 10(a) compares the two best solutions in the amplitude balance $E_1(\omega, \boldsymbol{x}^*)$ defined in (4). In Fig. 10(a), solid line denotes the amplitude balance achieved by the best solution of the extended optimum design problem. On the other hand, broken line denotes the amplitude balance achieved by the best solution of the original optimum design problem. Similarly, Fig. 10(b) compares the two best solutions in the phase balance $E_2(\omega, \boldsymbol{x}^*)$

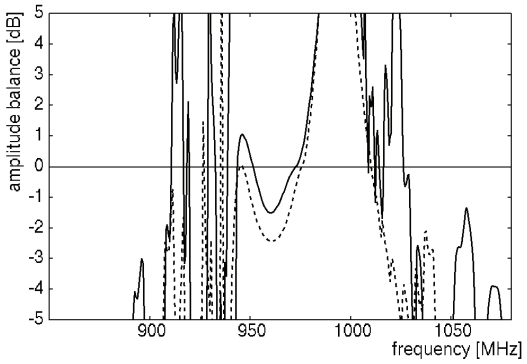

(a) Amplitude balance E_1

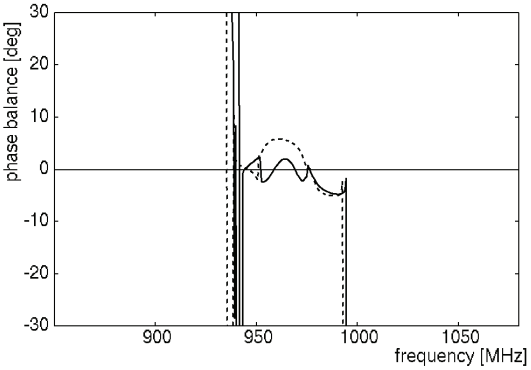

(b) Phase balance E_2

Fig. 10. Balance characteristics of the balanced SAW filter shown in Fig. 7

defined in (5). Comparing the solid lines with broken lines in Fig. 10, solid lines are closer to zero through the pass-band (*950~980*[MHz]). Therefore, from Fig. 10, we can say that the best solution of the extended optimum design problem is better than the best solution of the original optimum design in the balance characteristics of the balanced SAW filter.

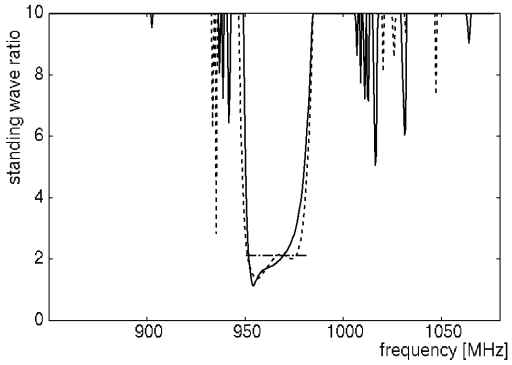

(a) Standing wave ratio of the output-port E_4

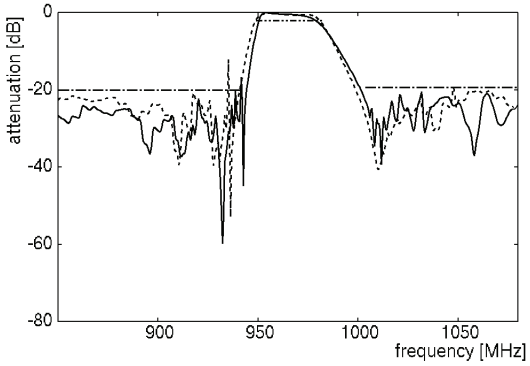

(b) Attenuation E_5

Fig. 11. Filter characteristics of the balanced SAW filter shown in Fig. 7

In the same way with Fig. 10, Fig. 11(a) compares the final best solution of the extended optimum design problem (*D=15*) with the final best solution of the original optimum design problem (*D=11*) in the standing wave ratio of the output-port $E_4(\omega, \boldsymbol{x}^*)$ defined in (10). Furthermore, Fig. 11(b) compares the two best solutions in the attenuation $E_5(\omega, \boldsymbol{x}^*)$ defined in (11). In Fig. 11, the upper bounds $U_r(\omega)$ of the respective criteria are denoted by one-broken lines. The lower bounds $L_r(\omega)$ of the respective criteria are also denoted by two-broken lines. Comparing the frequency response characteristics shown in Fig. 11, we cannot observe so much difference between the solid lines and the broken lines. In other words, as far as the band-pass filter characteristics, the performances of the balanced SAW filter achieved by the two best solutions resemble each other closely.

Consequently, from the comparison of the final best solution of the extended optimum design problem (*D=15*) with the final best solution of the original optimum design problem (*D=11*), we can say that the unsymmetrical structure of the balanced SAW filter has a capability to improve the balance characteristics of the conventional balanced SAW filter that has the symmetrical structure without losing the band-pass filter characteristics.

6. Conclusion

As an example of evolutionary computation technique in the real-world application, we presented an optimum design method for balanced SAW filters. First of all, in order to evaluate the performances of balanced SAW filters based on the computer simulation, we derived the network model of balanced SAW filters from the equivalent circuit model of them according to the balanced network theory. Then we formulated the structural design of balanced SAW filters as an optimization problem for improving their performances in both the balance characteristics and the filter characteristics. For solving the optimization problem, or the optimum design problem of balanced SAW filters, we employed DE. DE is a recent EA for solving real-parameter optimization problems. However, in the optimum design problem of balanced SAW filters, some design parameters take discrete values while others take continuous values. Therefore, in order to apply DE to the optimum design problem, we proposed a technique to insert the various design parameters of balanced SAW filters into the regularized continuous search space of DE. Finally, through the computational experiments conducted on a practical balanced SAW filter, we demonstrated the usefulness of the proposed optimum design method. Furthermore, we could obtain a new knowledge about the structural design of balanced SAW filters.

The balanced SAW filter usually takes a symmetrical structure. However, in the extended optimum design problem of the balanced SAW filter, we supposed that the balanced SAW filter could take an unsymmetrical structure. Then we compared the best solution of the extended optimum design problem with the best solution of the original optimum design problem. As a result, we found that the unsymmetrical structure of the balanced SAW filter could improve the balance characteristics without losing the filter characteristics.

If we increase the degree of the design freedom, or the number of design parameters, in the optimum design problem, the search space of DE is also expanded. As a result, the probability that DE finds the optimal solution decreases. On the other hand, the extended search space of DE may cover a new optimal solution that is better than the optimal solution in the original search space. In the optimum design of the balanced SAW filter, we could successfully increase the degree of the design freedom and utilize the power of DE.

Future work will focus on the revision of the classic DE used in this time. Since several variants of DE have been proposed (Chakraborty, 2008), we would like to compare their performances in the optimum design problems of various balanced SAW filters.

7. References

Bockelman, D. E. & Eisenstadt, W. R. (1995). Combined differential and common-mode scattering parameters: theory and simulation. *IEEE Transaction on Microwave Theory and Techniques,* Vol. 43, No. 7, pp. 1530-1539.

Campbell, C. K. (1998). *Surface Acoustic Wave Devices for Mobile and Wireless Communication,* Academic Press.

Chakraborty, U. K. (Edit) (2008). *Advances in Differential Evolution*, Springer.

Eshelman, L. J. & Schaffer, J. D. (1993). Real-coded genetic algorithms and interval-schemata, *Foundations Genetic Algorithms 2*, Morgan Kaufmann Publisher.

Franz, J.; Ruppel, C. C. W.; Seifert, F. & Weigel, R. (1997). Hybrid optimization techniques for the design of SAW filters, *Proceedings of IEEE Ultrasonics Symposium*, pp. 33-36.

Goto, S. & Kawakatsu, T. (2004). Optimization of the SAW filter design by immune algorithm, *Proceedings of IEEE International Ultrasonics Ferroelectrics, and Frequency Control Joint 50th Anniversary Conference*, pp. 600-603.

Hashimoto, K. (2000). *Surface Acoustic Wave Devices in Telecommunications – Modeling and Simulation,* Springer.

Kawachi, O.; Mitobe, S.; Tajima, M.; Yamaji, T.; Inoue, S. & Hashimoto, K. (2004). A low-pass and wide-band DMS filter using pitch-modulated IDT and reflector structures, *Proceedings of IEEE International Ultrasonics Ferroelectrics, and Frequency Control Joint 50th Anniversary Conference*, pp. 298-301.

Kojima, T. & Suzuki, T. (1992). Fundamental equations of electro-acoustic conversion for an interdigital surface-acoustic-wave transducer by using force factors. *Japanese Journal of Applied Physics Supplement,* No. 31, pp. 194-197.

Koshino, M.; Kanasaki, H.; Yamashita, T.; Mitobe, S.; Kawase, Y.; Kuroda, Y. & Ebata, Y. (2002). Simulation modeling and correction method for balance performance of RF SAW filters, *Proceedings of IEEE Ultrasonics Symposium*, pp. 301-305.

Meier, H.; Baier, T. & Riha, G. (2001). Miniaturization and advanced functionalities of SAW devices. *IEEE Transaction on Microwave Theory and Techniques,* Vol. 49, No. 2, pp. 743-748.

Meltaus, J.; Hamalainen, P.; Salomaa, M. & Plessky, V. P. (2004). Genetic optimization algorithms in the design of coupled SAW filters, *Proceedings of IEEE International Ultrasonics Ferroelectrics, and Frequency Control Joint 50th Anniversary Conference*, pp. 1901-1904.

Prabhu, V.; Panwar, B. S. & Priyanaka. (2002). Linkage learning genetic algorithm for the design of withdrawal weighted SAW filters, *Proceedings of IEEE Ultrasonics Symposium*, pp. 357-360.

Price, K. V.; Storn, R. M. & Lampinen, J. A. (2005). *Differential Evolution – A Practical Approach to Global Optimization*, Springer.

Storn, R and Price, K. (1997). Differential evolution – a simple and efficient heuristic for global optimization over continuous space, *Journal of Global Optimization*, Vol. 11, No. 4, pp. 341-359.

Tagawa, K.; Haneda, H.; Igaki, T. & Seki, S. (2002). Optimal design of three-IDT type SAW filter using local search, *Proceedings of the 28th Annual Conference of the IEEE Industrial Electronics Society*, pp. 2572-2577.

Tagawa, K.; Yamamoto, T.; Igaki, T. & Seki, S. (2003). An Imanishian genetic algorithm for the optimum design of surface acoustic wave filter, *Proceedings of the 2003 IEEE Congress on Evolutionary Computation*, pp. 2748-2755.

Tagawa, K.; Ohtani, T.; Igaki, T.; Seki, S. & Inoue, K. (2007). Robust optimum design of SAW filters by the penalty function method. *Electrical Engineering in Japan,* Vol. 158, No. 3, pp. 45-54.

Tagawa, K. (2007). Simulation modeling and optimization technique for balanced surface acoustic wave filters. *Proceedings of the 7th WSEAS International Conference on Simulation, Modelling and Optimization,* pp. 295-300.

Tagawa, K. (2008). Evolutionary computation techniques for the optimum design of balanced surface acoustic wave filters. *Proceedings of the 2008 IEEE Congress on Evolutionary Computation*, pp. 299-304.

Evolutionary Computation

Edited by Wellington Pinheiro dos Santos

ISBN 978-953-307-008-7
Hard cover, 572 pages
Publisher InTech
Published online 01, October, 2009
Published in print edition October, 2009

This book presents several recent advances on Evolutionary Computation, specially evolution-based optimization methods and hybrid algorithms for several applications, from optimization and learning to pattern recognition and bioinformatics. This book also presents new algorithms based on several analogies and metafores, where one of them is based on philosophy, specifically on the philosophy of praxis and dialectics. In this book it is also presented interesting applications on bioinformatics, specially the use of particle swarms to discover gene expression patterns in DNA microarrays. Therefore, this book features representative work on the field of evolutionary computation and applied sciences. The intended audience is graduate, undergraduate, researchers, and anyone who wishes to become familiar with the latest research work on this field.

INTECH
open science | open minds

InTech Europe
University Campus STeP Ri
Slavka Krautzeka 83/A
51000 Rijeka, Croatia
Phone: +385 (51) 770 447
Fax: +385 (51) 686 166
www.intechopen.com

InTech China
Unit 405, Office Block, Hotel Equatorial Shanghai
No.65, Yan An Road (West), Shanghai, 200040, China
中国上海市延安西路65号上海国际贵都大饭店办公楼405单元
Phone: +86-21-62489820
Fax: +86-21-62489821